Proc. Indian Acad. Sci. (*Chem. Sci.*), Vol. 115, Nos 5 & 6, October–December 2003, pp 473–490

Phase transitions in $A_4Li(HSO_4)_3(SO_4)$; A = Rb, K: Single crystal X-ray diffraction studies[¶]

G NALINI and T N GURU ROW*
Solid State and Structural Chemistry Unit, Indian Institute of Science,
Bangalore 560 012, India
e-mail: ssctng@sscu.iisc.ernet.in

Abstract. The crystal structure of ferroelastic $Rb_4Li(HSO_4)_3(SO_4)$ has been determined at two temperatures, which indicates a structural phase transition, tetragonal $P4_3$ with a = 7·629(1) Å, c = 29·497(2) Å at 293 K and monoclinic $P2_1$ with a = 7·583(3) Å, b = 29·230(19) Å, c = 7·536(5) Å, b = 90·14(1)° at 90 K. The crystal structure of $K_4Li(HSO_4)_3(SO_4)_4$ has also been determined at two temperatures, tetragonal $P4_1$ with a = 7·405(1) Å, c = 28·712(6) Å at 293 K and tetragonal $P4_1$ with a = 7·371(5) Å, c = 28·522(5) Å at 100 K. The overall coordination features in both the structures have been analysed in terms of bond valence sum calculations.

Keywords. Phase transition; ferroelastic; cryo-crystallography; crystal structure.

1. Introduction

Ferroelastic materials have been extensively reviewed[1–3] and they find application in the design of acoustic delay lines, transducers, optical shutters, modulators and as shape-memory materials. Compounds belonging to the family with general formula $A_4Li(HSO_4)_3(SO_4)$ where A = K, Rb exhibit ferroelastic properties[4]. These compounds at room temperature are generally found to display prototype tetragonal symmetry and undergo phase transitions at low temperatures and exhibit ferroelastic behaviour. Extensive physical studies including elastic, pyroelectric, dielectric and thermal measurements of this family of compounds suggest[5] that the pathway for phase transition from room temperature to low temperature could be either $4 \rightarrow 2$ type or $4 \rightarrow 2mm$ type. $Rb_4Li(HSO_4)_3(SO_4)$, hereafter RLHS and $K_4Li(HSO_4)_3(SO_4)$ hereafter KLHS have also been subjected to linear birefringence measurements[6] and EPR measurements.[7] In all these studies RLHS shows a well defined phase transition at $T_c \approx 122$ K (tetragonal to monoclinic) while the corresponding studies on KLHS though indicating the onset of transition at 110 K, does not exhibit recognizable changes in lattice parameters.[4] Also, thermal expansion studies on KLHS show no anomalies and the phase transition appears to be non ferroelastic.[8]

Single crystal studies on RLHS at room temperature (293 K) reported earlier[5] showed that the crystals are optically laevorotatory and belong to the enantiomorphous space group $P4_1$. However, an analysis of the diffraction data based on the value of enantiomorph polarity parameter during refinement suggested that the sample is 87% $P4_1$ and 13% $P4_3$. Initial photographic studies at 100 K, points to a reduction of symmetry from

[¶]Dedicated to Professor C N R Rao on his 70th birthday
*For correspondence

tetragonal to monoclinic system, if the transition is of ferrodistortive type within the framework of Landau theory.[5]

In order to ascertain the phase transition in RLHS unambiguously and to unequivocally establish the non-ferroelastic nature of the phase transition in KLHS, we have carried out detailed single crystal diffraction experiments. We describe here the details of these studies on RLHS and KLHS at room temperature (293 K), at 90 K for RLHS and at 100 K for KLHS respectively.

2. Experimental

Single crystals of both RLHS and KLHS were grown by slow evaporation at 313 K from an aqueous solution containing stoichiometric amounts of $Rb_2SO_4 : Li_2SO_4$ and $K_2SO_4 : Li_2SO_4$ in excess H_2SO_4 respectively. Beakers containing the solution (5 ml) were tightly corked to slow down the evaporation rate at this temperature. The crystals obtained were transparent, colourless and showed sharp optical extinction. The composition of the crystals was confirmed by preliminary powder X-ray diffraction as well as by EDAX measurements. The presence of the lithium ion was confirmed by qualitative chemical analysis. A variable temperature powder X-ray diffraction data collected on a STOE STADI-P diffraction system in the range 298 to 100 K using an Oxford cyrosystem nitrogen open-flow cryostat confirmed the phase transition for RLHS. The corresponding studies on KLHS show no change in the powder pattern in this range.

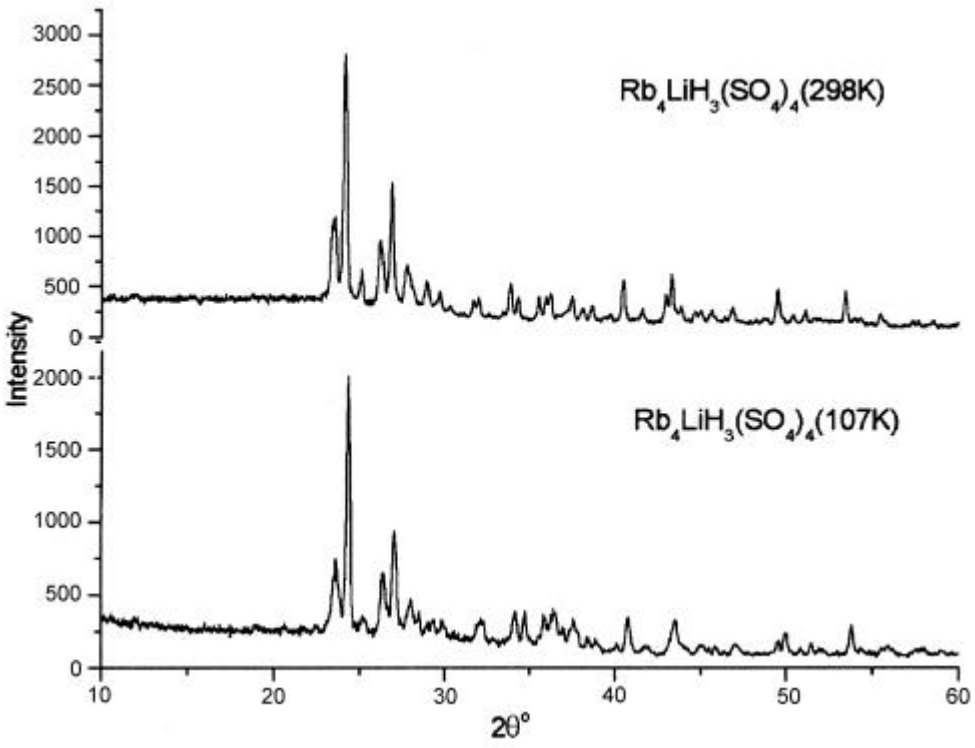

Figure 1. Powder X-ray diffraction pattern of RLHS at 298 and 107 K.

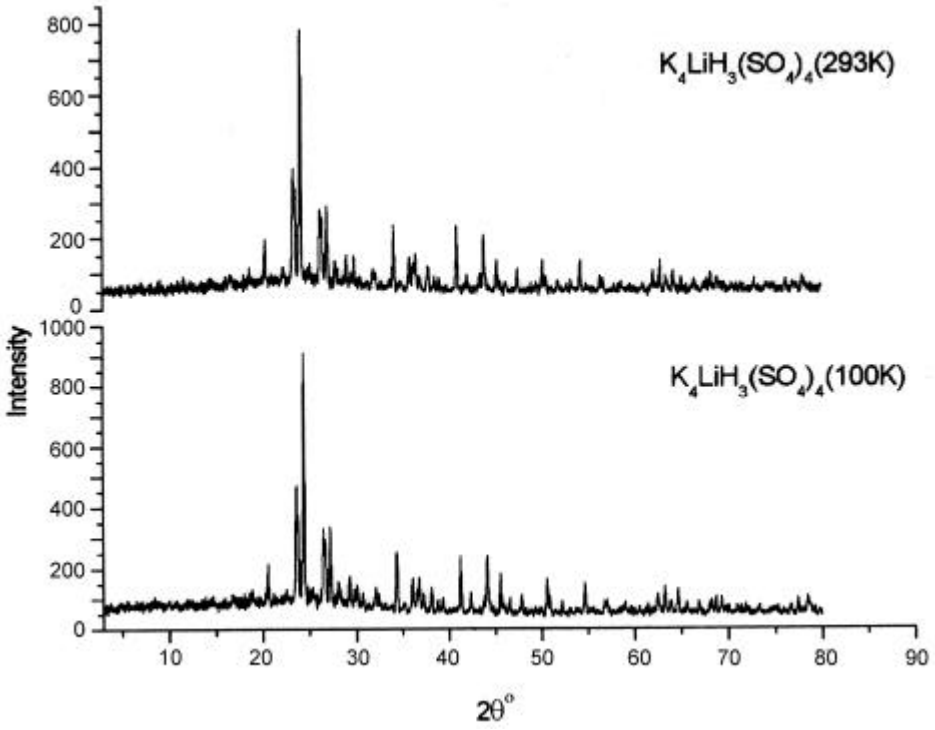

Figure 2. Powder X-ray diffraction pattern of KLHS at 298 and 100 K.

3. Structure determination and refinement

3.1 *Structure of RLHS at 293 K*

A crystal of size 0·7 × 0·3 × 0·4 mm was mounted on a BRUKER AXS SMART APEX CCD[9] diffractometer with a crystal to detector distance of 6·03 cm. The diffraction intensities were measured with monochromated MoK_a radiation (λ = 0·7107 Å). The orientation matrix of the crystal was obtained at room temperature from reflections derived from 50 frames to give the tetragonal unit cell (table 1). The data was collected in four batches covering a complete sphere of reciprocal space with each batch at different φ angles (φ = 0, 90, 180, 270) and each frame covering 0·3° in ω at 10 s exposure time. The data were 98·7% complete to 56° in 2θ. As it is important to fix the handedness of this enantiomorphous space group the structure determination and refinement were carried out in both $P4_1$ and $P4_3$. The positional coordinates of Rb and S atoms were obtained by direct methods using the SHELXS97[10] module and refined by SHELXL97[10] in the WinGX[11] suite of software. Subsequent difference Fourier synthesis revealed the positions of the remaining non-hydrogen atoms. It was observed that S1–O12, S2–O23 and S3–O34 bonds were long in the sulphate tetrahedra indicating the presence of hydrogen atoms. More ever, the oxygen atoms O12, O23 and O34 showed O…O short contacts signifying the presence of hydrogen bonds. Hence, the hydrogen atoms were geometrically fixed on O12, O23 and O34 restricting the O to H distance to 0·97 Å which is the average neutron length found from a statistical analysis of data from CSD[12]. The

details of the refinements are given in table 1. Refinement in $P4_1$ space group converged with the Flack parameter[13] = 1·03(2), $R = 0{\cdot}070$, $wR = 0{\cdot}177$ with a residual density of 0·978 e/Å^3 and the corresponding values for the refinements in space group $P4_3$ are Flack parameter = – 0·001(1),[13] $R = 0{\cdot}043$, $wR = 0{\cdot}104$ and residual density = 0·932 e/Å^3. It is thus conclusive that RLHS indeed belongs to the space group $P4_3$. The residual densities are clustered around Rb atoms (table 1). There is no disorder in the sulphate moiety. The final coordinates along with the equivalent thermal parameters are listed in table 2a.

Table 1. Crystal data, measurements, and structure refinement parameters for $Rb_4Li(HSO_4)_3SO_4$).

Temperature	293 K	90 K
(i) *Crystal data*		
Empirical formula	$Rb_4Li(HSO_4)_3(SO_4)$	$Rb_4Li(HSO_4)_3(SO_4)$
Crystal habit	Block	Block
Crystal colour	Colourless	Colourless
Crystal size* (mm)	0·7 × 0·3 × 0·4	0·7 × 0·3 × 0·4
Crystal system	Tetragonal	Monoclinic
Space group	$P4_3$	$P2_1$
Cell dimensions (Å)	a = 7·629(1) c = 29·497(2)	a = 7·583(3) b = 29·230(19) c = 7·536(5) b = 90·14(1)
Volume (Å^3)	1715·81(2)	1670·74(1)
Formula weight	736·1	736·1
Density (calculated) (g/cm^3)	2·85	2·93
Z	4	4
F (000)	1384	1384
Flack parameter	–0·001(9)	0·07(1)
(ii) *Data collection*		
Equipment	BRUKER APEX SMART CCD	BRUKER APEX SMART CCD
l (MoKa (graphite monochromator)) (Å)	0·7107	0·7107
Scan mode	w	w
q range (°)	2·7–27·3	2·7–28
Recording reciprocal space	$-9 \rightarrow h \rightarrow 9$ $-9 \rightarrow k \rightarrow 9$ $-37 \rightarrow l \rightarrow 37$	$-8 \rightarrow h \rightarrow 9$ $-30 \rightarrow k \rightarrow 38$ $-8 \rightarrow l \rightarrow 9$
No. of measured reflections	36891	9270
No. of independent reflections	3734	6393
m (mm^{-1})	11·90	11·90
Absorption correction	SADABS	SADABS
Data reduction	SAINT	SAINT
(iii) *Refinement*		
No. of refined parameters	228	452
Refinement method	Full matrix least squares	Full matrix least squares
R [$I > 2sI$]/R [all data]	0·043/0·051	0·061/0·073
WR [$I > 2sI$]/R [all data]	0·104/0·106	0·146/0·151
GoF	1·08	1·07
Max/min Δr eÅ^{-3}	0·935/–0·79	1·68/–1·38

*The same crystal is used for both the data sets

3.2 *Structure of RLHS at 90 K*

The same crystal used for the room temperature data was cooled to 90 K at a ramp rate of 120 K/h and left to stabilise for 60 min (about 30 K below T_c; reported $T_c = 122$ K[6]). An Oxford Cryosystem nitrogen open-flow cryostat was used to maintain the temperature of 90 K through out the data collection within ± 0·2 K. The space group was uniquely determined as $P2_1$ from systematic absences with $\boldsymbol{b} = 90{\cdot}14°$ (table 1). The positional coordinates of Rb and S atoms obtained from direct methods were refined and the subsequent difference Fourier synthesis revealed the positions of the remaining non-hydrogen atoms in the structure. The longer bonds [S1A–O12A = 1·540(10); S2A–O12B = 1·554(10); S2A–O23A = 1·577(10); 2B–O23B = 1·566(11); S3A–O34A = 1·546(10); S3B–O34B = 1·536(10)] are again characteristic of the presence of the hydrogen atoms. The oxygen atoms O12A, O12B, O23A, O23B, O34A, O34B show

Table 2a. Fractional atomic coordinates and equivalent thermal parameters (U_{eq}) for $Rb_4LiH_3(SO_4)_4$ at 293 K.

$U_{eq} = -(2p^2(U_{11}(h.a^*))^2 + (U_{22}(k.b^*))^2 + (U_{33}(l.c^*))^2 + 2.U_{12}.h.k.a^*.b^* + 2U_{12}h.l.a^*.c^* + 2.U_{23}.k.l.b^*.c^*)$

Atom	*x*	*y*	*z*	U_{eq} (Å)^2
Rb(1)	0·8854(1)	0·9356(1)	0·2253(1)	0·0276(2)
Rb(2)	0·7727(1)	0·5189(1)	0·1197(1)	0·0279(2)
Rb(3)	1·3801(1)	0·6350(1)	0·2382(1)	0·0301(2)
Rb(4)	0·4709(1)	1·0251(1)	0·1099(1)	0·0290(2)
S(1)	0·4097(2)	1·1229(3)	0·2372(1)	0·0209(4)
S(2)	0·8751(2)	0·4619(2)	0·2387(1)	0·0194(2)
S(3)	1·3029(2)	0·5377(2)	0·1102(1)	0·0209(4)
S(4)	0·9637(2)	1·0045(2)	0·1067(1)	0·0196(4)
O(11)	0·3434(8)	1·2547(8)	0·2063(2)	0·0318(15)
O(12)	0·2548(8)	1·0265(8)	0·2509(2)	0·0348(14)
O(13)	0·5093(9)	1·2071(10)	0·2734(2)	0·0488(20)
O(14)	0·5111(9)	0·9930(9)	0·2131(3)	0·0436(17)
O(21)	1·0233(8)	0·5593(8)	0·2561(2)	0·0356(15)
O(22)	0·7437(8)	0·5726(8)	0·2179(2)	0·0307(13)
O(23)	0·7899(8)	0·3780(8)	0·2813(2)	0·0339(15)
O(24)	0·9232(7)	0·3179(7)	0·2085(2)	0·0327(13)
O(41)	0·8330(9)	0·8934(8)	0·1279(2)	0·0366(14)
O(42)	1·0868(7)	1·0721(8)	0·1408(2)	0·0323(13)
O(43)	1·0686(9)	0·9142(9)	0·0709(2)	0·0441(18)
O(44)	0·8693(8)	1·1574(8)	0·0850(2)	0·0329(14)
O(31)	1·1556(8)	0·4886(8)	0·1373(2)	0·0381(15)
O(32)	1·4023(8)	0·3930(8)	0·0925(2)	0·0364(15)
O(34)	1·2313(8)	0·6263(8)	0·0669(1)	0·0393(16)
O(33)	1·4115(10)	0·6649(8)	0·1330(8)	0·0329(14)
Li(1)	1·1285(15)	1·2769(16)	0·1728(5)	0·0264(23)
H(12)	0·2288	1·0782	0·2884	0·05[#]
H(23)	0·6832	0·3166	0·2726	0·05[#]
H(34)	1·1516	0·7205	0·0748	0·05[#]

[#]Hydrogen atom coordinates and isotropic thermal parameters are fixed during refinements

Table 2b. Fractional atomic coordinates and equivalent thermal parameters (U_{eq}) for $Rb_4LiH_3(SO_4)_4$ at 90 K.

Atom	*x*	*y*	*z*	U_{eq} (Å)^2
Rb(1A)	1·0109(2)	– 0·0449(1)	0·2319(2)	0·0183(3)
Rb(1B)	1·0317(2)	0·1943(1)	– 0·0189(2)	0·0202(3)
Rb(2A)	0·6167(2)	0·3089(1)	0·0689(2)	0·0173(3)
Rb(2B)	1·3604(2)	0·0724(1)	0·6189(2)	0·0193(3)
Rb(3A)	0·7349(2)	0·2051(1)	0·4882(1)	0·0180(3)
Rb(3B)	0·4811(2)	0·4441(1)	0·4717(2)	0·0200(3)
Rb(4A)	0·1192(2)	0·3226(1)	0·3642(2)	0·0187(3)
Rb(4B)	1·4306(2)	0·0586(1)	1·1163(2)	0·0174(3)
S(1A)	1·0927(5)	0·3217(1)	– 0·1228(5)	0·0179(7)
S(1B)	1·2001(5)	0·1940(1)	0·4654(5)	0·0159(7)
S(2A)	0·9601(5)	0·0735(1)	0·1282(4)	0·0164(7)
S(2B)	1·0337(5)	– 0·0558(1)	0·6996(5)	0·0166(7)
S(3A)	0·6277(5)	0·3234(1)	0·5419(5)	0·0161(7)
S(3B)	1·6193(5)	0·0719(1)	0·5889(5)	0·0178(7)
S(4A)	0·4992(5)	0·4408(1)	– 0·0359(5)	0·0204(8)
S(4B)	0·5412(5)	0·1905(1)	0·0011(5)	0·0185(8)
O(11A)	1·1633(16)	0·2916(4)	– 0·2577(15)	0·0304(26)
O(12A)	1·2478(14)	0·3433(4)	– 0·0201(15)	0·0243(24)
O(13A)	0·9926(18)	0·3588(4)	– 0·2035(4)	0·0439(37)
O(14A)	0·9875(15)	0·2970(4)	0·0072(14)	0·0237(24)
O(11B)	1·3542(15)	0·2205(4)	0·5212(13)	0·0229(24)
O(12B)	1·2687(16)	0·1500(3)	0·3733(14)	0·0250(26)
O(13B)	1·1003(15)	0·1761(4)	0·6125(14)	0·0221(23)
O(14B)	1·0922(15)	0·2176(4)	0·3417(13)	0·0305(24)
O(21A)	1·0715(14)	0·0526(4)	0·2592(15)	0·0214(22)
O(22A)	0·8119(15)	0·0439(4)	0·0792(13)	0·0219(23)
O(23A)	0·8792(15)	0·1179(3)	0·2135(13)	0·0231(25)
O(24A)	1·0586(14)	0·0915(4)	– 0·0212(13)	0·0211(23)
O(21B)	0·8865(14)	– 0·0734(4)	0·6014(13)	0·0214(23)
O(22B)	1·1601(14)	– 0·0334(4)	0·5891(15)	0·0216(23)
O(23B)	1·1238(15)	– 0·0999(4)	0·7744(15)	0·0271(26)
O(24B)	0·9810(15)	– 0·0286(4)	0·8511(14)	0·0252(25)
O(31A)	0·5812(14)	0·2933(4)	0·6885(13)	0·0226(23)
O(32A)	0·4785(13)	0·3408(4)	0·4424(15)	0·0229(23)
O(33A)	0·7592(15)	0·3034(4)	0·4288(15)	0·0255(23)
O(34A)	0·7111(14)	0·3665(3)	0·6257(15)	0·0253(26)
O(31B)	1·7566(15)	0·0431(4)	0·6555(15)	0·0262(25)
O(32B)	1·6916(19)	0·1096(4)	0·4827(20)	0·0390(33)
O(33B)	1·4925(16)	0·0463(4)	0·4924(16)	0·0227(23)
O(34B)	1·5214(15)	0·0935(4)	0·7462(15)	0·0258(26)
O(41A)	0·4140(14)	0·2249(3)	– 0·0621(12)	0·0179(22)
O(42A)	0·4350(14)	0·4762(4)	0·0868(14)	0·0209(22)
O(43A)	0·6170(14)	0·4613(4)	– 0·1695(17)	0·0252(24)
O(44A)	0·5890(17)	0·4044(4)	0·0675(19)	0·0373(31)
O(41B)	0·3455(14)	0·4193(3)	– 0·1287(13)	0·0200(22)
O(42B)	0·6758(14)	0·2120(4)	0·1133(13)	0·0201(21)
O(43B)	0·4465(20)	0·1540(4)	0·0959(16)	0·0374(33)
O(44B)	0·6323(14)	0·1692(3)	– 0·1544(14)	0·0198(22)
Li(1)	0·7728(33)	0·0076(10)	– 0·1245(35)	0·0283(65)
Li(2)	0·3761(39)	0·2566(10)	– 0·2720(34)	0·0311(68)
H(12A)	0·7225	0·8728	0·0708	0·05[#]
H(12B)	1·3643	0·1573	0·2930	0·05[#]
H(23A)	0·8092	0·1099	0·3165	0·05[#]
H(23B)	0·7678	0·4087	0·1653	0·05[#]
H(34A)	0·8104	0·3599	0·6998	0·05[#]
H(34B)	1·5699	0·0026	0·8123	0·05[#]

[#]Hydrogen atom coordinates and isotropic thermal parameters are fixed during refinements

O…O short contacts signifying the presence of hydrogen bonds. The hydrogen atoms were thus geometrically fixed by restricting the O to H distance[12] to 0·97 Å. The details of the refinements are given in table 1. The refinement for $P2_1$ space group converged with the Flack parameter = 0·07(1),[13] $R = 0{\cdot}061$, $wR = 0{\cdot}146$ with a residual density of 1·68 e/Å^3. The coordinates along with the equivalent thermal parameters are listed in table 2b.

Table 3. Crystal data, measurement, and structure refinement parameters for $K_4Li(HSO_4)_3(SO_4)$.

Temperature	293 K	100 K
(i) *Crystal data*		
Empirical formula	$K_4Li(HSO_4)_3(SO_4)$	$K_4Li(HSO_4)_3(SO_4)$
Crystal habit	Block	Block
Crystal colour	Colourless	Colourless
Crystal size* (mm)	0·1 × 0·1 × 0·4	0·1 × 0·1 × 0·4
Crystal system	Tetragonal	Tetragonal
Space group	$P4_1$	$P4_1$
Cell dimensions (Å)	a = 7·405(1)	a = 7·371(1)
	c = 28·712(6)	c = 28·522(5)
Volume (Å^3)	1574·39(4)	1549·5(4)
Formula weight	550·6	550·6
Density (calculated) (g/cm^3)	2·32	2·36
Z	4	4
F (000)	1096	1096
Flack parameter	0·02(4)	0·03(7)
(ii) *Data collection*		
Equipment	Bruker APEX SMART CCD	Bruker APEX SMART CCD
l (MoKa (graphite monochromator)) (Å)	0·7107	0·7107
Scan mode	w	w
q range (°)	2·8–27·5	2·8–27·5
Recording reciprocal space	$-9 \rightarrow h \rightarrow 9$	$-9 \rightarrow h \rightarrow 7$
	$-9 \rightarrow k \rightarrow 9$	$-9 \rightarrow k \rightarrow 9$
	$-37 \rightarrow l \rightarrow 37$	$-37 \rightarrow l \rightarrow 29$
No. of measured reflections	17390	8296
No. of independent reflections	3624	3195
m (mm^{-1})	1·74	1·74
Absorption correction	SADABS	SADABS
Data reduction	SAINT	SAINT
(iii) *Refinement*		
No. of refined parameters	238	238
Refinement method	Full matrix least squares	Full matrix least squares
R [$I > 2sI$]/R [all data]	0·030/0·031	0·039/0·047
WR [$I > 2sI$]/R [all data]	0·072/0·073	0·083/0·086
GoF	1·15	1·06
Max/min Δr eÅ^{-3}	0·342/–0·682	0·40/–0·474

*The same crystal is used for both the data sets

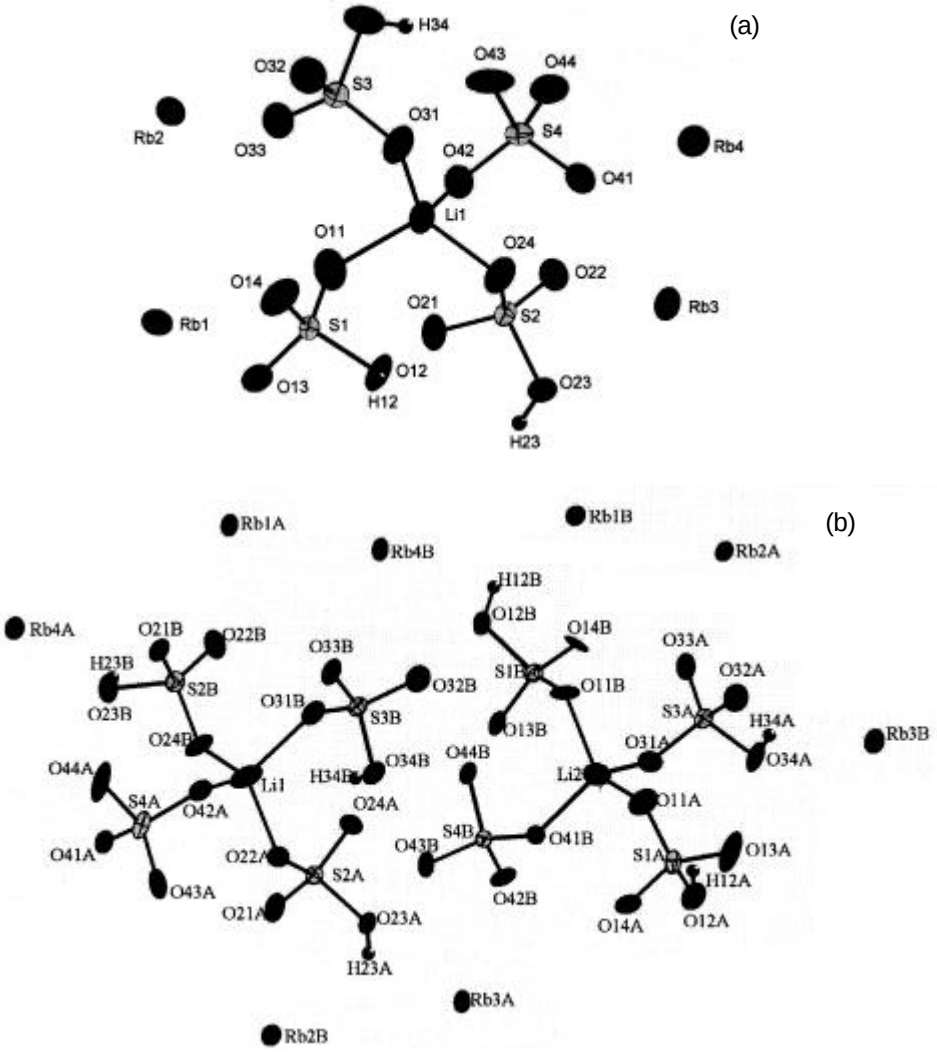

Figure 3. (**a**) and (**b**) ORTEP diagram of RLHS (293 and 90 K) at 50% probability level.

3.3 *Structure of KLHS at 293 K*

Intensity data were collected on a BRUKER AXS SMART APEX CCD[9] diffractometer at the Chemistry Department in the University of Durham. A crystal of size 0·1 × 0·1 × 0·4 mm was mounted. The diffraction intensities were measured with monochromated MoK_a radiation ($\lambda = 0{\cdot}7107$ Å). The crystal structure was solved by direct methods using the SHELXS97[10] module in the WinGX[11] suite of software. It is important to fix the handedness of this enantiomorphous space group and hence the structure determination and refinement were carried out in both $P4_1$ and $P4_3$ respectively. The positional coordinates of K and S atoms obtained direct methods were refined and the subsequent difference Fourier synthesis revealed the positions of the remaining non-hydrogen atoms

in the structure. The coordinates of hydrogen atoms located from the difference Fourier map were isotropically refined. The details of the refinements are given in table 3. Refinement in $P4_1$ space group converged with the Flack parameter = 0·02(4),[13] $R = 0{\cdot}03$, $wR = 0{\cdot}072$ with the residual density of 0·342 e/Å^3 and the corresponding values for the refinements in space group $P4_3$ are Flack parameter = 0·98(6),[13] $R = 0{\cdot}033$, $wR = 0{\cdot}086$ and residual density = 0·537 e/Å^3. Therefore KLHS was assigned the space group $P4_1$. The residual densities are clustered around K atoms (table 3). There is no disorder in the sulphate moiety. The coordinates along with the equivalent thermal parameters are listed in table 4a.

3.4 *Structure of KLHS at 100 K*

The same crystal used for the room temperature data was cooled to 100 K (about 10 K below T_c; reported $T_c = 110$ K[7] using an Oxford Cryosystem nitrogen open-flow cryostat. The temperature of 100 K was maintained through out the data collection. At 100 K KLHS does not show any phase transition and retains the tetragonal symmetry. The diffraction intensities were measured with monochromated MoK$_a$ radiation (λ =

Table 4a. Fractional atomic coordinates and equivalent thermal parameters (U_{eq}) for $K_4LiH_3(SO_4)_4$ at 293 K.

Atom	x	y	z	U_{eq} (Å)^2
K(1)	0·5104(2)	0·0146(2)	0·0232(1)	0·0302(2)
K(2)	– 0·3755(1)	0·3991(1)	– 0·1018(1)	0·030(2)
K(3)	0·0964(1)	– 0·0807(1)	0·1343(1)	0·0126(2)
K(4)	0·2132(1)	– 0·4938(1)	0·0336(1)	0·0264(2)
S(1)	0·4522(1)	– 0·1090(1)	– 0·0099(1)	0·0184(1)
S(2)	0·1083(1)	0·4283(1)	– 0·0995(1)	0.0191(2)
S(3)	0·0207(1)	– 0·0091(1)	0·0173(1)	0·0186(2)
S(4)	– 0·3227(1)	– 0·4729(1)	0·0216(1)	0·0197(1)
O(11)	0·3753(4)	– 0·1867(4)	– 0·0538(1)	0·0311(6)
O(12)	0·5661(4)	– 0·2451(3)	– 0·1212(1)	0·0297(5)
O(13)	0·5534(4)	0·0467(3)	– 0·0840(1)	0·0331(6)
O(14)	0·2980(3)	– 0·0678(4)	– 0·1295(1)	0·0304(6)
O(21)	0·0091(4)	0·2643(3)	– 0·0798(1)	0·0292(5)
O(22)	0·2507(4)	0·3656(4)	– 0·1301(1)	0·0381(7)
O(23)	0·1845(4)	0·5264(4)	– 0·0599(1)	0·0415(8)
O(24)	– 0·0238(4)	0·5332(4)	– 0·1245(1)	0·0375(7)
O(31)	– 0·1136(3)	0·0465(3)	0·0520(1)	0·0303(6)
O(32)	0·1554(3)	– 0·1221(4)	0·0390(1)	0·0297(6)
O(33)	– 0·0684(4)	– 0·0996(4)	– 0·0220(1)	0·0356(7)
O(34)	0·1142(4)	0·1559(3)	– 0·0018(1)	0·0299(6)
O(41)	– 0·4324(4)	– 0·3408(4)	0·0457(1)	0·0335(6)
O(42)	– 0·2535(4)	– 0·3887(4)	– 0·0249(1)	0·0325(6)
O(43)	– 0·1632(4)	– 0·5196(4)	0·0483(1)	0·0337(6)
O(44)	– 0·4255(4)	– 0·6275(4)	0·0061(1)	0·0355(6)
Li(1)	– 0·1487(7)	– 0·7348(8)	0·0840(3)	0·0261(9)
H(11)	0·328(6)	– 0·271(6)	– 0·061(2)	0·042(15)[#]
H(34)	0·053(9)	0·209(9)	– 0·042(2)	0·087(27)[#]
H(42)	– 0·203(6)	– 0·296(6)	– 0·183(2)	0·048(14)[#]

[#]Hydrogen atoms were refined isotropically

Table 4b. Fractional atomic coordinates and equivalent thermal parameters (U_{eq}) for $K_4LiH_3(SO_4)_4$ at 100 K.

Atom	*x*	*y*	*z*	U_{eq} (Å)^2
K(1)	0·5109(1)	0·0098(2)	0·0236(1)	0·0146(2)
K(2)	– 0·3745(2)	0·3968(2)	– 0·1024(1)	0·0141(2)
K(3)	0·0969(2)	– 0·0861(2)	0·1333(1)	0·0126(2)
K(4)	0·2182(1)	– 0·5012(1)	0·0345(1)	0·0121(2)
S(1)	0·4510(2)	– 0·1105(2)	– 0·0099(1)	0·0105(3)
S(2)	0·1064(2)	0·4279(2)	– 0·0991(1)	0·0105(3)
S(3)	0·0216(2)	– 0·0136(2)	0·0170(1)	0·0097(3)
S(4)	– 0·3207(2)	– 0·4774(2)	0·0211(1)	0·0105(2)
O(11)	0·3744(5)	– 0·1882(5)	– 0·0527(1)	0·0141(8)
O(12)	0·5646(5)	– 0·2490(5)	– 0·1213(1)	0·0144(8)
O(13)	0·5539(5)	0·0466(5)	– 0·0846(1)	0·0149(8)
O(14)	0·2936(5)	– 0·0706(5)	– 0·1289(1)	0·0138(8)
O(21)	0·0057(5)	0·2621(5)	– 0·0796(1)	0·0128(8)
O(22)	0·2550(5)	0·3631(5)	– 0·0261(1)	0·0150(8)
O(23)	0·1787(6)	0·5266(5)	– 0·0586(1)	0·0191(9)
O(24)	– 0·0257(5)	0·5300(5)	– 0·1253(1)	0·0204(8)
O(31)	– 0·1141(5)	0·3957(5)	0·0520(1)	0·0151(8)
O(32)	0·1575(5)	– 0·1301(5)	0·0383(1)	0·0192(8)
O(33)	– 0·0688(5)	– 0·1029(5)	– 0·0227(1)	0·0178(9)
O(34)	0·1147(5)	0·1542(5)	– 0·0013(1)	0·0145(8)
O(41)	– 0·4307(5)	– 0·3444(5)	0·0457(1)	0·0154(8)
O(42)	– 0·2566(5)	– 0·3927(6)	– 0·0261(1)	0·0150(8)
O(43)	– 0·1584(5)	– 0·5250(5)	0·0474(1)	0·0149(8)
O(44)	– 0·4253(5)	– 0·6336(5)	0·0061(1)	0·01626(8)
Li(1)	– 0·1471(11)	– 0·7404(10)	0·0846(4)	0·0128(14)
H(11)	0·268(8)	– 0·315(9)	– 0·060(21)	0·031(30)[#]
H(34)	0·088(11)	0·189(11)	– 0·025(3)	0·052(27)[#]
H(42)	– 0·224(9)	– 0·312(9)	– 0·190(3)	0·017(19)[#]

[#]Hydrogen atoms were refined isotropically

Table 5. Selected bond lengths (Å) and bond valence sum at 293 K for $Rb_4Li(HSO_4)_3(SO_4)$ ($P4_3$).

S(1)–O(11)	1·448(7)	S(3)–O(31)	1·431(7)
S(1)–O(12)	1·531(7)	S(3)–O(32)	1·437(7)
S(1)–O(13)	1·456(7)	S(3)–O(33)	1·443(7)
S(1)–O(14)	1·445(8)	S(3)–O(34)	1·548(6)
Valence sum	6·06	*Valence sum*	6·20
S(2)–O(21)	1·445(7)	S(4)–O(41)	1·450(7)
S(2)–O(22)	1·446(6)	S(4)–O(42)	1·470(6)
S(2)–O(23)	1·549(6)	S(4)–O(43)	1·463(7)
S(2)–O(24)	1·460(6)	S(4)–O(44)	1·515(6)
Valence sum	6·03	*Valence sum*	6·00
Li(1)–O(42)	1·85(1)	Li(1)–O(31)	1·93(1)
Li(1)–O(11)	1·92(1)	Li(1)–O(24)	1·91(1)

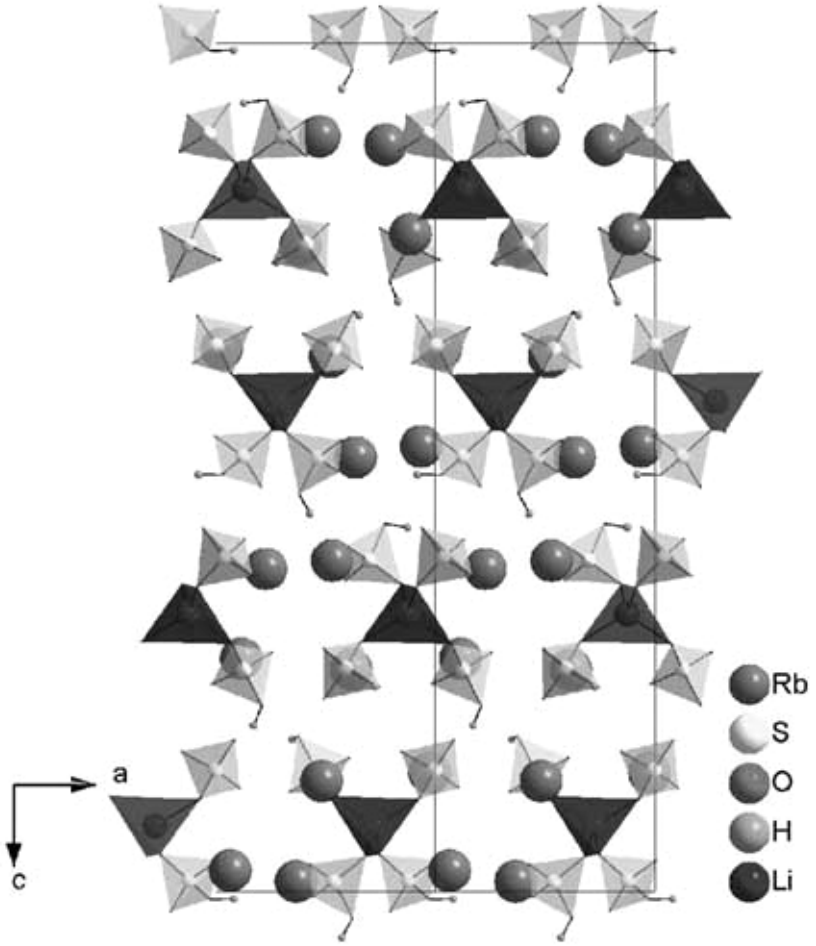

Figure 4. Packing diagram of RLHS at 293 K.

0·7107 Å). The crystal structure was solved by direct methods using the SHELXS97[10] module in the WinGX[11] suite of software in the space group $P4_1$. The positional coordinates of K and S atoms obtained from initial *E*-map based on direct methods were refined and the subsequent difference Fourier synthesis revealed the positions of the remaining non-hydrogen atoms in the structure. The details of the refinements are given in table 3. The coordinates of hydrogen atoms located from the difference Fourier map were isotropically refined. The coordinates along with the equivalent thermal parameters are listed in table 4b.

4. Results and discussion

4.1 *Structure of RLHS*

Selected bond lengths[14] and bond valence sum[15] are given in tables 3 and 4 for the room temperature and 90 K structures respectively. The ORTEP[16] with 50% probability ellip-

soids are given in figure 3a and b. Figures 4 and 5 give the corresponding packing diagrams.[16]

The room temperature structure of RLHS displays one large S–O distance in each of the four sulphate tetrahedra. The hydrogen atoms were thus fixed stereochemically on these oxygen atoms. The structure is made up of layers of Rb atoms perpendicular to the four-fold screw axis (figure 4). The lithium atoms intercalated between these layers form a tetrahedra by sharing oxygen atoms from each of the four independent sulphate tetrahedra. The Li–O bonds range from 1·85 to 1·93 Å (table 5). It is interesting to note that there are no O–H…O hydrogen bonds even though the corresponding intermolecular

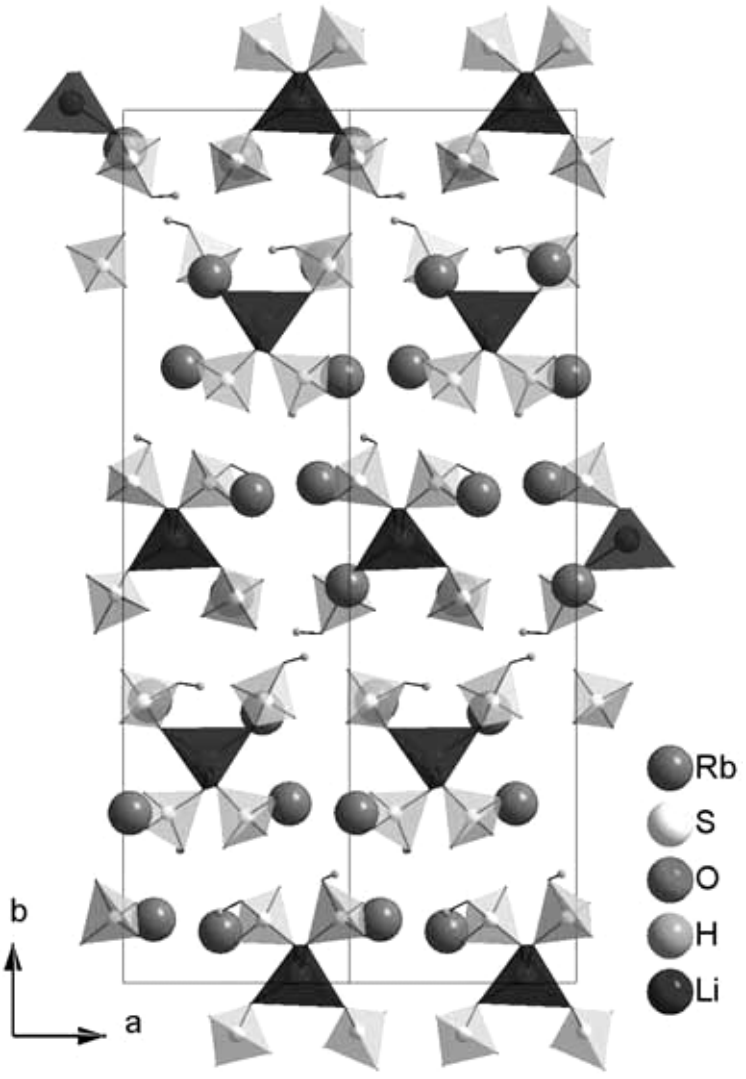

Figure 5. Packing diagram of RLHS at 90 K.

oxygen atoms are at 2·55 Å. There are eight oxygen atoms coordinating with the Rb atoms and the bond valence sums (table 5) indicate regular bonding features.

The ferroelastic phase of RLHS results due to a small lattice distortion of the prototype, and hence at the microscopic level in the unit cell, there are pairs of atomic positions for the atoms of the same element, which retain the pseudo symmetry with small shifts in the atom positions. These small shifts result in the long and short S–O bonds. The structure of RLHS at 90 K has large deviations in the geometry of the sulphate tetrahedra. Indeed, the S–O distances vary from 1·418 Å (12) to 1·571 (11) Å (table 6) suggesting significant distortions in the sulphate moieties. These distortions

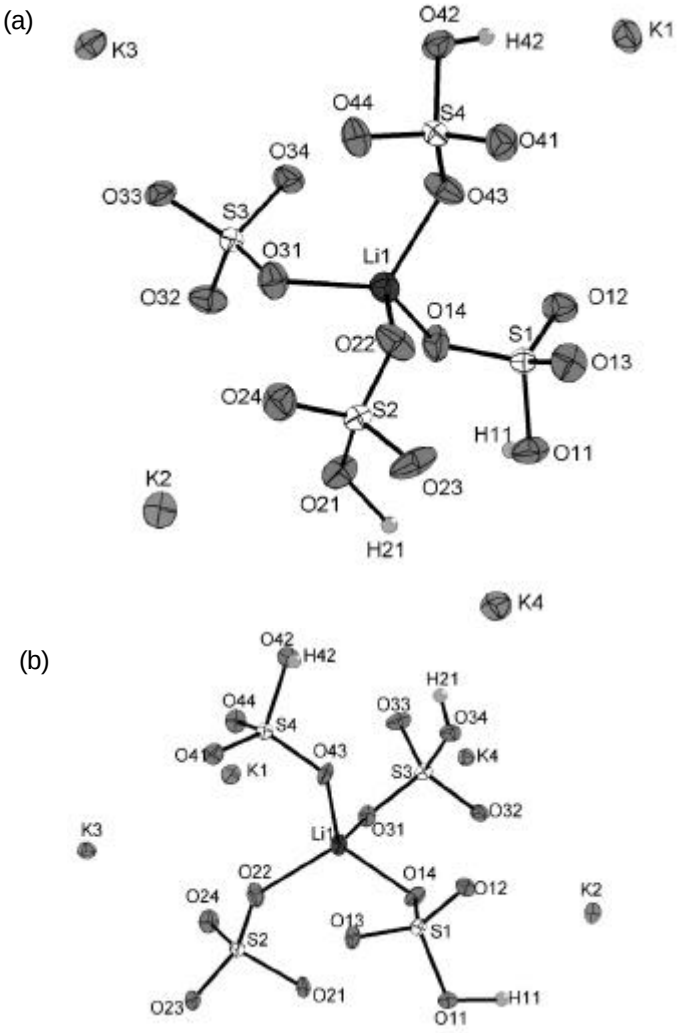

Figure 6. (**a**) and (**b**) ORTEP diagram for KLHS (293 and 100 K) at 50% probability level.

could be the cause of the strain in the lattice resulting in the compound exhibiting ferroelasticity. The bond valence sums (table 6) reflect on the distortions developed due to the structural phase transitions. The hydrogen atoms were fixed stereochemically once again on the longer S–O bonds. The gross features associated with the Rb layers; the Li coordination and the overall packing characteristics remain similar. There is no change in the Rb coordination.

4.2 *Structure of KLHS*

Selected bond lengths[14] and bond valence sum[15] are given in table 5 for the room temperature and 100 K structures. The ORTEP[16] with 50% probability ellipsoids are given in figures 6a and b, while figures 7 and 8 give the corresponding packing diagrams.[16]

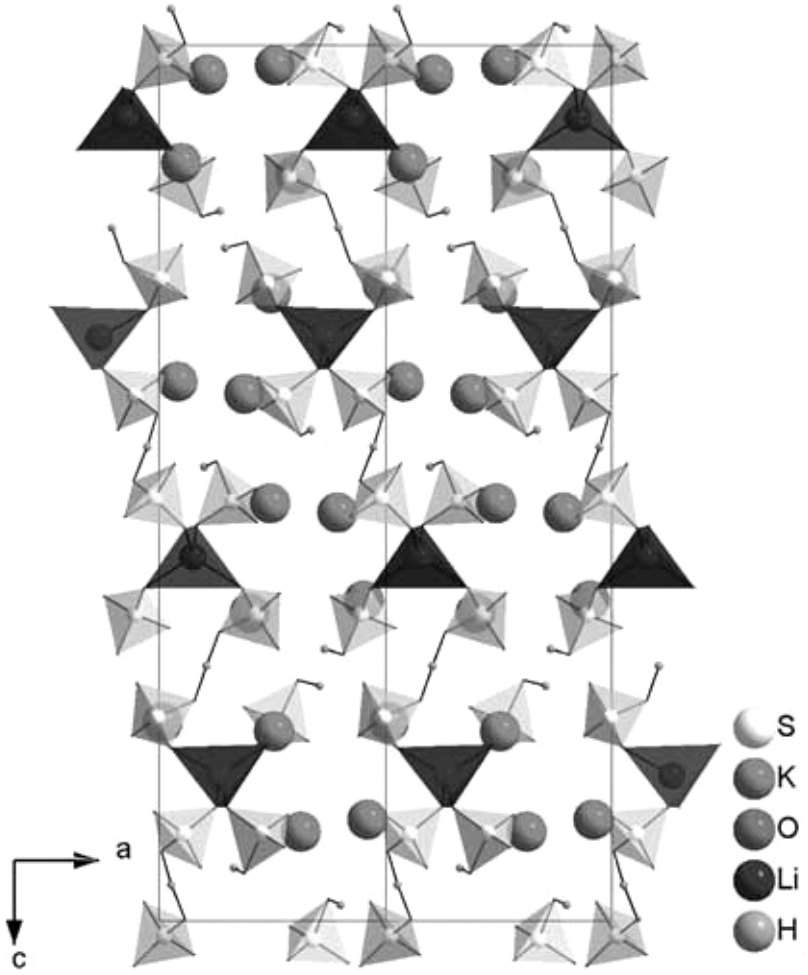

Figure 7. Packing diagram of KLHS at 293 K.

The room temperature structure of KLHS has features similar to those observed in RLHS. However, the hydrogen atoms could be located from difference Fourier maps and refined isotropically. The Li atom forms a tetrahedron by sharing oxygen atoms from each of the four sulphate tetrahedral. The Li–O bonds range from 1·885(7) to 1·930(7) (table 7). KLHS displays three very strong, well-defined classical O–H…O hydrogen bonds (table 8). The sulphate moieties are linked by these hydrogen bonds (figure 7). The K atoms are 8 coordinated. There are no distortions in the sulphate moiety as found in RLHS accompanying the phase transition. One of the hydrogen bonds O34…H34…O21 is almost covalent at 293 K as found by charge density analysis of compounds containing very strong O–H…O bonds.[17] The bond valence sums (table 7) indicate regular bonding features.

The low temperature structure of KLHS shows no structural phase transition. However, the hydrogen-bonding pattern at 293 and 100 K differs significantly. The

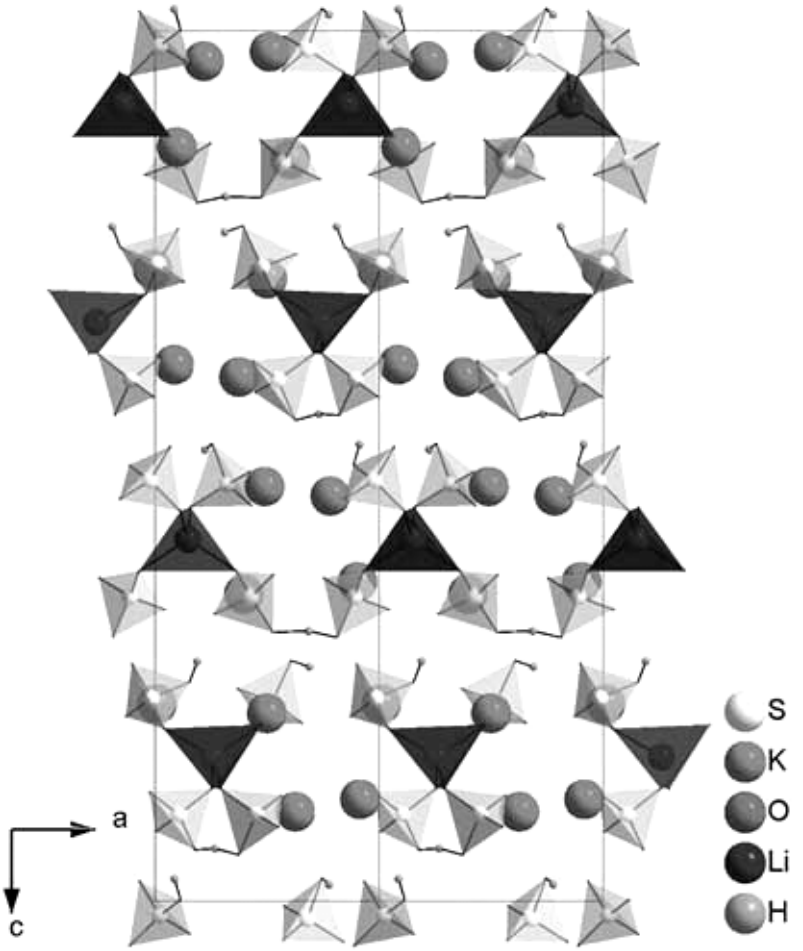

Figure 8. Packing diagram of KLHS at 100 K.

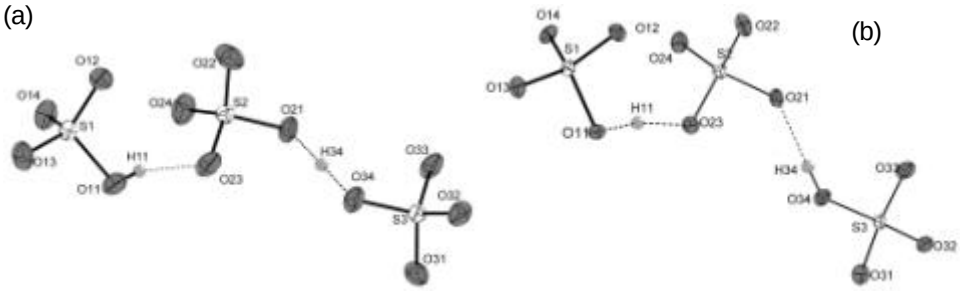

Figure 9. (**a**) and (**b**) Significant migration of proton in the short strong hydrogen bond at 293 and 100 K in KLHS.

Table 6. Selected bond lengths and bond valence sum (Å) at 90 K for $Rb_4Li(HSO_4)_3(SO_4)$ ($P2_1$).

S(1A)–O(11A)	1·466(11)	S(3A)–O(31A)	1·456(11)
S(1A)–O(12A)	1·540(11)	S(3A)–O(32A)	1·447(11)
S(1A)–O(13A)	1·455(14)	S(3A)–O(33A)	1·438(12)
S(1A)–O(14A)	1·456(11)	S(3A)–O(34A)	1·546(11)
Valence sum	6·07	*Valence sum*	5·94
S(1B)–O(11B)	1·463(12)	S(3B)–O(31B)	1·429(12)
S(1B)–O(12B)	1·554(11)	S(3B)–O(32B)	1·468(13)
S(1B)–O(13B)	1·442(12)	S(3B)–O(33B)	1·418(12)
S(1B)–O(14B)	1·420(11)	S(3B)–O(34B)	1·536(11)
Valence sum	6·13	*Valence sum*	6·15
S(2A)–O(21A)	1·435(11)	S(4A)–O(41A)	1·495(11)
S(2A)–O(22A)	1·467(11)	S(4A)–O(42A)	1·469(11)
S(2A)–O(23A)	1·571(11)	S(4A)–O(43A)	1·475(12)
S(2A)–O(24A)	1·452(11)	S(4A)–O(44A)	1·483(13)
Valence sum	5·96	*Valence sum*	5·87
S(2B)–O(21B)	1·434(11)	S(4B)–O(43B)	1·472(12)
S(2B)–O(22B)	1·432(11)	S(4B)–O(44B)	1·497(11)
S(2B)–O(23B)	1·566(11)	S(4B)–O(41B)	1·472(11)
S(2B)–O(24B)	1·448(11)	S(4B)–O(42B)	1·467(11)
Valence sum	6·27	*Valence sum*	6·08
Li(1)–O(22A)	1·89(2)	Li(2)–O(11A)	1·90(3)
Li(1)–O(42A)	1·84(2)	Li(2)–O(11B)	1·89(2)
Li(1)–O(31B)	1·95(2)	Li(2)–O(31A)	1·91(3)
Li(1)–O(24B)	1·91(3)	Li(2)–O(41B)	1·85(3)

centre of gravity of the protons H11 and H34 alters with temperature as shown in figure 9a and b. The transformation from a dissymmetrical O–H…O electrostatic interaction to a covalent and symmetrical O–H–O bond has been reported both by X-ray diffraction and neutron diffraction extensively in literature.[18–20] It can be observed from table 6 that the

distance of the disymmetric O11–H11 bond has increased from 0·74 Å at 293 K to 1·24 Å at 100 K, while the symmetric O34…H34…O21 bond (1·24 Å) at 293 K becomes the dissymmetric O34–H34 (0·75 Å) at 100 K due to the migration of the protons H11 and H34. Hence the near covalent feature associated with the hydrogen bond O34…H34…O21 at 293 K has completely shifted to another hydrogen bond O11…H11…O23 at 100 K (table 8). Thus, even though in accordance to thermal expansion studies, there is no

Table 7. Selected bond lengths (Å) and bond valence sum for $K_4Li(HSO_4)_3(SO_4)$ ($P4_1$) at 293 and 100 K.

Bond length	293 K	100 K
S(1)–O(11)	1·546(3)	1·553(4)
S(1)–O(12)	1·451(3)	1·463(4)
S(1)–O(13)	1·448(3)	1·445(3)
S(1)–O(14)	1·458(3)	1·464(4)
Valence sum	5·87	6·00
S(2)–O(21)	1·527(3)	1·534(4)
S(2)–O(22)	1·452(3)	1·469(4)
S(2)–O(23)	1·461(3)	1·464(4)
S(2)–O(24)	1·442(3)	1·440(3)
Valence sum	6·97	6·08
S(3)–O(31)	1·460(3)	1·467(4)
S(3)–O(32)	1·443(3)	1·453(4)
S(3)–O(33)	1·470(3)	1·471(4)
S(3)–O(34)	1·509(3)	1·509(4)
Valence sum	6·08	6·08
S(4)–O(41)	1·443(3)	1·451(4)
S(4)–O(42)	1·558(3)	1·559(4)
S(4)–O(43)	1·456(3)	1·455(4)
S(4)–O(44)	1·445(3)	1·453(4)
Valence sum	5·94	6·02
Li(1)–O(43)	1·896(7)	1·912(9)
Li(1)–O(22)	1·910(7)	1·900(9)
Li(1)–O(14)	1·930(7)	1·929(9)
Li(1)–O(31)	1·885(7)	1·884(1)

Table 8. Hydrogen bonding scheme in $K_4Li(HSO_4)_3(SO_4)$.

Temp (K)	D–H…A (Å)	D–H (Å)	H…A (Å)	D…A (Å)	D–H…A (°)
293	O(11)–H(11)…O(23)	0·74(5)	1·84(5)	2·557(4)	162(5)
293	O(34)–H(34)…O(21)	1·24(6)	1·27(6)	2·500(2)	174(2)
293	O(42)–H(42)…O(33)	0·82(5)	1·75(5)	2·543(4)	163(5)
100	O(11)–H(11)…O(23)	1·24(7)	1·34(7)	2·555(5)	164(5)
100	O(34)–H(34)…O(21)	0·75(8)	1·75(9)	2·501(5)	179(12)
100	O(42)–H(42)…O(33)	0·67(7)	1·92(7)	2·543(6)	154(7)

structural phase transition observed in KLHS, there is migration of protons at 100 K resulting in the shortening and lengthening of hydrogen bonds. It has been explained that the change in the EPR spectra of KLHS at 110 K,[7] could be either due to the sulphate tetrahedron system or in the cationic subsystem, since the sulphate radicals may exhibit their own dynamics. It can be conjectured that the dynamics of the sulphate radicals can be a direct consequence of the dynamics of the proton subsystem, which has a weak influence on the parameters of the crystal structure. This could be the microscopic change observed in the EPR spectra.

5. Conclusion

Phase transition studies by single crystal X-ray diffraction indicate that the low temperature behaviour of RLHS and KLHS are different. RLHS undergoes a structural phase transition at 90 K to a monoclinic space group $P2_1$. The distortions in the sulphate moieties at 90 K turn out to be the key features inducing the ferroelastic phase transition. The absence of structural phase transition in KLHS is confirmed. A striking feature is the formation of a strong short hydrogen bond O34–H34 and migration of the hydrogen atom H11 towards the mid-point of the hydrogen bond resulting in the switching of the covalent nature from one hydrogen bond to another on cooling to 100 K.

Acknowledgments

Data collection on the DST sponsored CCD facility under the IRPHA-DST program. The data sets for KLHS were collected at University of Durham and we acknowledge the help from Prof. J A K Howard and Dr Ivana R Evans G N thanks Council of Scientific and Industrial Research, New Delhi for a fellowship.

References

1. Wadhawan V K 1984 *Bull. Mater. Sci.* **6** 733
2. Wadhawan V K 1991 *Phase Transitions* **34** 3
3. Guymont M 1991 *Phase Transitions* **34** 135
4. Piskunowicz P, Breczewski T and Wolejko T 1989 *Phys. Stat. Sol.* **A114** 505
5. Zuniga F J, Etxebarria J, Madriaga G and Breczewski T 1990 *Acta Crystallogr.* **C46** 1199
6. Przeslawski J, Glazer A M and Czapla Z 1990 *Solid State Commun.* **74** 1165
7. Minge J and Krajewski T 1988 *Phys. Stat. Sol.* **A109** 193
8. Mroz B and Laiho R 1989 *Phys. Stat. Sol.* **A115** 575
9. Bruker 1998 SMART and SAINT. Bruier AXS Inc., Madison, Wisconsin, USA
10. Sheldrick G M 1997 SHELXS97, SHELXL97, University of Gottingen, Germany
11. Farrugia L J 1997 *J. Appl. Crystallogr.* **30** 565
12. Allen F H 1986 *Acta Crystallogr.* **A42** 515
13. Flack H D 1983 *Acta Crystallogr.* **A39** 876
14. Nardelli M 1995 *J. Appl. Crystallogr.* **28** 659
15. Hormillosa C 1993 Institute For Materials Research, McMaster University, Version 2.00
16. Pennington W T 1999 *J. Appl. Crystallogr.* **32** 1028
17. Stevens E D and Coppens P 1980 *Acta Crystallogr.* **B36** 1864
18. Wilson C C 2001 *Acta Crystallogr.* **B57** 435
19. Steiner T, Majerz I and Wilson C C 2001 *Angew. Chem., Int. Ed.* **40** 2651
20. Sooryanarayana K and Guru Row T N 1996 *Phase Transitions* **58** 263